Available online at www.sciencedirect.com
SCIENCE DIRECT®
Biomaterials 24 (2003) 4265–4272
Biomaterials
www.elsevier.com/locate/biomaterials

Fiber templating of poly(2-hydroxyethyl methacrylate) for neural tissue engineering

Lauren Flynn[a,b], Paul D. Dalton[a,b], Molly S. Shoichet[a,b,c,*]

[a] Department of Chemical Engineering and Applied Chemistry, University of Toronto, 200 College Street, Toronto, Ont., Canada M5S 3E5
[b] Institute of Biomaterials and Biomedical Engineering, University of Toronto, 4 Taddle Creek Road, Toronto, Ont., Canada M5S 3G9
[c] Department of Chemistry, University of Toronto, 80 St. George Street, Toronto, Ont., Canada M5S 3H6

Received 13 November 2002; accepted 8 April 2003

Abstract

We have developed a method to create longitudinally oriented channels within poly(2-hydroxyethyl methacrylate) (pHEMA) hydrogels for neural tissue engineering applications. Incorporated into an entubulation strategy, these scaffolds have the potential to enhance nerve regeneration after transection injuries of either the spinal cord or the peripheral nerve by increasing the available surface area and providing guidance to extending axons and invading cells. The fabrication process is straightforward and the resultant scaffolds are highly reproducible. Polycaprolactone (PCL) fibers were extruded and embedded in transparent, crosslinked pHEMA gels. Sonication of the pHEMA/PCL composite in acetone resulted in the complete dissolution of the PCL, leaving longitudinally oriented, fiber-free channels in the pHEMA gel. Regulating the size and quantity of the PCL fibers allowed us to control the diameter and number of channels. Small and large channel scaffolds were fabricated and thoroughly characterized. The small channel scaffolds had 142 ± 7 channels, with approximately 75% of the channels in the 100–200 μm size range. The large channel scaffolds had 37 ± 1 channels, with approximately 77% of the channels in the 300–400 μm range. The equilibrium water content (EWC), porosity and compressive modulus were measured for each of the structures. Small and large channel scaffolds had, respectively, EWCs of $55.0\pm1.2\%$ and $56.2\pm2.9\%$, porosities of $35\pm1\%$ and $40\pm1\%$ and compressive moduli of 191 ± 7 and 182 ± 4 kPa.

Keywords: pHEMA; Polycaprolactone; Fibers; Spinal cord injury; Regeneration; Nerve guidance channel; Scaffold; Orientation; Hydrogel

1. Introduction

Nerve injury is debilitating in both the peripheral nervous system (PNS), where regeneration is limited to small gaps [1], and the central nervous system (CNS), where regeneration is essentially non-existent due to both physical (i.e. glial scar) and chemical (i.e. myelin proteins) inhibitors [2,3]. The standard treatment for peripheral nerve injury across gaps greater than a few millimeters involves the use of autografts, nerve tissue taken from a donor site and grafted into the injured site [4]. However, this strategy is frequently associated with donor site morbidity and incomplete functional recovery. To improve on these results, several laboratories are investigating the use of tubes, or nerve guides, to bridge the gap between transected nerves in both the CNS and PNS. Of the numerous entubulation studies reported to date, some of the best results have been achieved in the PNS over short distances with nerve guides consisting of poly(glycolic acid) [5], poly(caprolactone-co-lactic acid) [6] and collagen [7].

We have been actively pursuing synthetic alternatives to replace the autograft for use in transection injury treatment strategies in either the PNS or CNS. To this end, we have developed a new methodology to produce hollow fiber membranes [8,9] and have begun to test these devices in vivo with some success [10–12]. In order to further enhance recovery, we hypothesize that regeneration will be augmented by the inclusion of a scaffold that increases surface area and provides both haptotactic [13] and chemotactic cues [14,15]. The focus of this paper is on the creation of longitudinally oriented

*Corresponding author. Department of Chemical Engineering and Applied Chemistry, University of Toronto, 200 College Street, Toronto, Ont., Canada M5S 3E5. Tel.: +1-416-978-1460; fax: +1-416-978-4317.
E-mail address: molly@ecf.utoronto.ca (M.S. Shoichet).

0142-9612/03/$ - see front matter © 2003 Elsevier Science Ltd. All rights reserved.
doi:10.1016/S0142-9612(03)00334-X

porous scaffolds that will fill the interior of a nerve guidance channel. We expect that this scaffold will provide greater surface area and directionality to regenerating nerve fibers.

To achieve our goals for an oriented scaffold, we wanted to design a structure that would support the systems' natural pattern of growth [16] which, in the spinal cord, for example, consists of the natively oriented ascending sensory pathways and descending motor pathways. Longitudinally oriented scaffolds would meet the biological requirements of physically supporting and guiding regenerating fibers within the tube and ultimately aid in functional recovery. Others have followed a similar strategy for enhanced regeneration in the past, using, for example, filaments of: aligned collagen [17–19], carbon [20], poly(L-lactide) [21] or polyamide [22]. In each of these strategies, longitudinal orientation was achieved with fibers. While nerve regeneration over long peripheral nerve gaps improved with these fiber-filled devices versus empty tubes [23,24], possibly due to increased surface area, the arrangement of the filaments within the guidance channels was irregular and difficult to reproduce. We propose a different approach to the fiber-filled tube—a scaffold with microtubular architecture, where regenerating axons extend through open longitudinal channels, as they would normally extend through endoneurial tubes of a peripheral nerve. This latter strategy promises to be more effective and reproducible.

Of the wide diversity of materials available, we chose to work with synthetic hydrogel scaffolds because they have been used in several biomedical applications due to their versatile nature [25–27]. Hydrogels are soft and flexible, exhibiting physical characteristics similar to those of soft tissue. Poly(2-hydroxyethyl methacrylate) (pHEMA) is particularly attractive for biomedical engineering applications because its physical properties can be easily manipulated through formulation chemistry [28] and it has been used extensively in medical applications, such as contact lenses, keratoprostheses and as orbital implants [29–32]. Furthermore, a pHEMA scaffold could be easily incorporated into the nerve guidance tubes that we have already developed as a part of our entubulation repair strategy [9].

We describe herein a new and facile method for the creation of longitudinally oriented channels in pHEMA gels using a fiber templating technique. Biodegradable polycaprolactone (PCL) fibers were extruded and embedded in transparent pHEMA gels, leading to the creation of a pHEMA-PCL composite. The PCL fibers were removed by dissolution resulting in longitudinal, fiber-free channels distributed in the pHEMA. The fibers' dimensions controlled those of the channels, as was demonstrated with two fiber types, leading to pHEMA gels having either small or large longitudinal channels. Based on previous studies examining the role of fiber diameter on guidance in vitro [33], we chose to create channels having the majority of pores between 100 and 200 μm (small channels). To demonstrate the versatility of this technique, we also made scaffolds with channels having the majority of pores between 300 and 400 μm (large channels). Ultimately, cell-adhesive peptides and/or growth-promoting neurotrophins could be incorporated into this scaffolding structure to further enhance regeneration [14,34].

2. Materials and methods

2.1. Materials

All chemicals were purchased from Aldrich Chemical Co. (Milwaukee, WI) and used as received. Water was distilled and deionized using a Millipore Milli-RO 10 Plus filtration system at 18 MΩ resistance.

2.2. Polymerization

HEMA was polymerized at room temperature in a glass tubular mold, with an inner diameter of 4.0 mm, which was capped at both ends with rubber septa. HEMA was polymerized by a redox-initiator in the presence of a crosslinking agent in an aqueous solution. The formulation consisted of: 60 wt% HEMA, 0.5 wt% ammonium persulfate (APS), 0.4 wt% tetramethylethylene diamine (TEMED), 0.1 wt% ethylene dimethacrylate (EDMA) crosslinker, and 40 wt% aqueous solution, of which 90 wt% was water and 10 wt% was ethylene glycol (EG). The APS, TEMED and EDMA concentrations are expressed as weight percentages of the total monomer concentration. A 10 wt% aqueous solution of APS initiator was prepared prior to every use. This formulation resulted in transparent pHEMA gels, facilitating visual analysis of the channels within the resultant structures.

2.3. Fiber extrusion

A high-pressure piston extruder with a fixed orifice of 0.3 mm (SpinLine, DACA Instruments) was used to form fibers from PCL pellets having a weight average molar mass of 80,000 g/mol. The pellets were melted in the heated 10 ml barrel at 67°C for 2 h prior to extrusion to ensure a consistent molten solution and thereby minimize air bubbles in the molten polymer. The force exerted by the piston and the speed of the winder controlled the diameter of the fibers produced. Two different sizes of fibers were extruded in order to create scaffolds with different channel diameters. To fabricate small diameter fibers, the piston advanced at a rate of 1.0 mm/min and the winder speed was set at 2.5 m/min.

For the larger diameter fibers, the piston speed was 1.6 mm/min and the winder speed was 0.8 m/min.

2.4. Scaffold fabrication

Two different types of scaffolds were created—small channel and large channel—based on the size of the extruded PCL fibers. After extrusion, the fibers were removed from the winder, grouped into bundles of like fiber diameter and then fused by melting the ends of the strands together with a Bunsen burner. The PCL bundles were inserted into 4.0 mm ID glass tubing, threaded through with the fused end first. The ends of the bundles were trimmed and the tubes sealed with rubber septa. For each sample, the relevant quantities of HEMA, water and EG were placed in an amber vial and the monomer mixture was degassed under vacuum. The appropriate quantities of initiator and accelerating agent were added to the vial and the mixture was agitated gently for 30 s. The mixture was then injected into the fiber-filled polymerization mold, displacing all of the air within the vessel. Polymerization proceeded for a minimum of 8 h, after which the pHEMA/PCL composites were removed from the glass tubing and immersed in distilled water until the next stage of processing.

The polymerized samples were cut into 1 cm long sections and placed in scintillation vials filled with acetone. The vials were sonicated for 75 min, resulting in the complete dissolution of the PCL fibers in the solvent. The samples were then removed from the vial and rinsed 3 times with fresh acetone to remove any residual PCL. The etched scaffolds were Soxhlet extracted in water for 12 h to remove residual acetone, followed by immersion in distilled water for a minimum of 24 h.

2.5. Structural characterization

Optical microscopy and scanning electron microscopy (SEM) were used to characterize the scaffolds for channel count, channel diameter and scaffold porosity. To create contrast for optical microscopy, the scaffolds were stained with 0.4% Giemsa methanol stain and then immediately washed in water. For SEM imaging, the samples were cut to the required mounting sizes, quenched in liquid nitrogen and then freeze-dried. Dried scaffolds were then attached with carbon paint to microscopy sample studs and sputter-coated with gold for 60 s. The samples were then placed on the SEM stage (Model S-570, Hitachi) for imaging. Operating conditions included a working distance of 15 mm and an accelerating voltage of 20 kV to minimize damage to the polymer structure.

2.5.1. Channel count

The number of channels present in each type of scaffold was counted from the SEM micrographs. A total of six different samples of each type, small channel and large channel, were analyzed to calculate an average and standard deviation in channel number.

2.5.2. Channel diameter

The diameters of the channels were measured from SEM micrographs using Scion Image Analysis 4.0.2 software. A total of 5 different samples of each type of scaffold were analyzed. In the small channel samples, approximately 130 channels per specimen were measured to obtain a size distribution. In the large channel samples, approximately 30 channels were measured. Averages and standard deviations are reported.

2.5.3. Scaffold porosity

The porosity of each type of scaffold was calculated using stereomicroscopic images of Giemsa-stained cross-sections, to clearly identify the channels within each structure by differentiating between the background and the gel phase. Scion Image Analysis 4.0.2 software was utilized to measure the surface area of the entire scaffold. The staining of the scaffold facilitated the use of the thresholding function in this software package to determine the surface area of only the gel portion of the scaffold, excluding the area occupied by the channels. The porosity was calculated according to the following equation:

$$\text{Porosity} = \frac{A_{\text{scaffold}} - A_{\text{gel}}}{A_{\text{scaffold}}} \times 100\%, \quad (1)$$

where A_{scaffold} is the surface area of the entire scaffold, including channels, and A_{gel} is the surface area of the gel only. Three samples of each type of scaffold were analyzed at 3 different points along their length. By calculating the porosity at various points within the same sample, it was possible to assess scaffold uniformity and channel continuity within the structures. Hence, a total of 9 different porosity measurements were obtained for each type of scaffold. The averages and standard deviations are reported.

2.6. Equilibrium water content

For equilibrium water content (EWC) measurements of the scaffolds following acetone fiber etching, five samples of each scaffold type were placed in deionized water, exchanged daily, for 2 weeks. The residual surface water was then removed and each sample was weighed to measure the hydrated scaffold mass. The samples were then dehydrated at 50°C over a 2-week period. Each scaffold was then re-weighed to ascertain the dry mass. The EWC was calculated according to the following equation:

$$\text{EWC} = \frac{(w_{\text{h}} - w_{\text{d}})}{w_{\text{h}}} \times 100\% \quad (2)$$

where w_h is the hydrated and w_d the dry mass of the scaffolds.

2.7. Compressive modulus

The elastic (Young's) modulus of each type of scaffold was assessed using a micro-mechanical tester (Dynatek Delta). All tests were conducted in triplicate, with 20% compression of 2.5 mm length sections over a 180 s time interval. This ensured results within the linear range of behavior for the material. The load was applied parallel to the longitudinal architecture of the channels. The samples were placed in an aqueous chamber during the testing procedure to maintain hydration of the scaffold. The cross-sectional area of the entire scaffold was measured using a stereomicroscope. Additionally, the modulus of the gel-phase portion of each scaffold was calculated. For this procedure, the cross-sectional area was determined through structural analysis of stereomicroscope images using Scion Image Analysis 4.0.2. The measured area included only the gel phase of each scaffold, with the area occupied by the empty channels excluded from the calculation. Based on previous studies, the expected value for the modulus of transparent pHEMA gels was approximately 290 kPa [35].

3. Results and discussion

The primary goal of this investigation was to design and characterize a scaffold with oriented, longitudinal channels that would provide increased surface area within a tubular structure for use in neural tissue engineering applications. Such a scaffold could support and guide extending axons subsequent to nerve injury in a cell-adhesive scaffold. We chose to create an oriented scaffold using pHEMA gels because we had shown that pHEMA tubes were conducive to cell-penetration in vivo [10,12]. Furthermore, by working with high HEMA concentrations, we could create transparent gels that facilitated characterization.

To develop a safe, effective and reproducible method for scaffold formation, we used a chemical dissolution technique for the creation of fiber-free longitudinally oriented channels in transparent pHEMA. By varying the diameter of the extruded fibers, scaffolds of differing channel diameters were formed. PCL, unlike poly(lactic acid) and poly(lactic-co-glycolic acid), was particularly appropriate to use in this method because PCL was insoluble in HEMA yet soluble in acetone. The acetone, used to dissolve the PCL fibers, did not significantly swell the pHEMA gel, and the crosslinked polymer maintained good structural integrity during the acetone washing process. As summarized in Table 1, fiber diameter influenced channel count the most, varying from 37 for large diameter fibers to 142 for small diameter fibers.

The optical and electron micrographs revealed that the scaffolds were consistent along the longitudinal axis, with the channels distributed throughout the gel phase portion of the scaffolds. Fig. 1 shows representative images of the two types of scaffolds produced. There was no evidence to suggest merging of individual channels, indicating that there was good wetting of the PCL fibers by the monomer mixture during the polymerization/fabrication process. Further, the gel provided sufficient support to prevent structural collapse following fiber dissolution. Visual analysis confirmed longitudinally oriented, fiber-free channels running throughout the transparent pHEMA gel.

3.1. Channel count

The number of channels within each scaffold (small and large) was consistent and reproducible between batches. The ends of the thermoplastic PCL fibers were melted together to form bundles, which could be easily introduced into the glass mold prior to the injection of the HEMA monomer formulation. For extruded fibers of similar diameter, modulating the packing density of the fiber bundles within the glass molds controlled channel count. Thus, by filling the molds to capacity with the fibers, there was little variation in the number of channels per sample. In the small diameter channel samples, an average of 142 ± 7 channels were present per sample. Due to the increase in fiber diameter in the large channel samples, the packing density of fibers was significantly lower and consequently easier to control. In the large diameter channel samples, an average of 37 ± 1 channels were present per sample.

The ability to control both the size and density of the channels may be important to the success of the scaffold. In neural applications, for example, it may be

Table 1
Comparison of the physical properties of scaffolds created with small fibers and large fibers in terms of number of channels, equilibrium water content, porosity and compressive modulus (average and standard deviation are reported)

Channels	Channel count (#, $n = 6$)	Equilibrium water content (%, $n = 5$)	Porosity (%, $n = 3$)	Compressive modulus (kPa, $n = 3$)
Small	142 ± 7	55.0 ± 1.2	35 ± 1	191 ± 7
Large	37 ± 1	56.2 ± 2.9	40 ± 1	182 ± 4

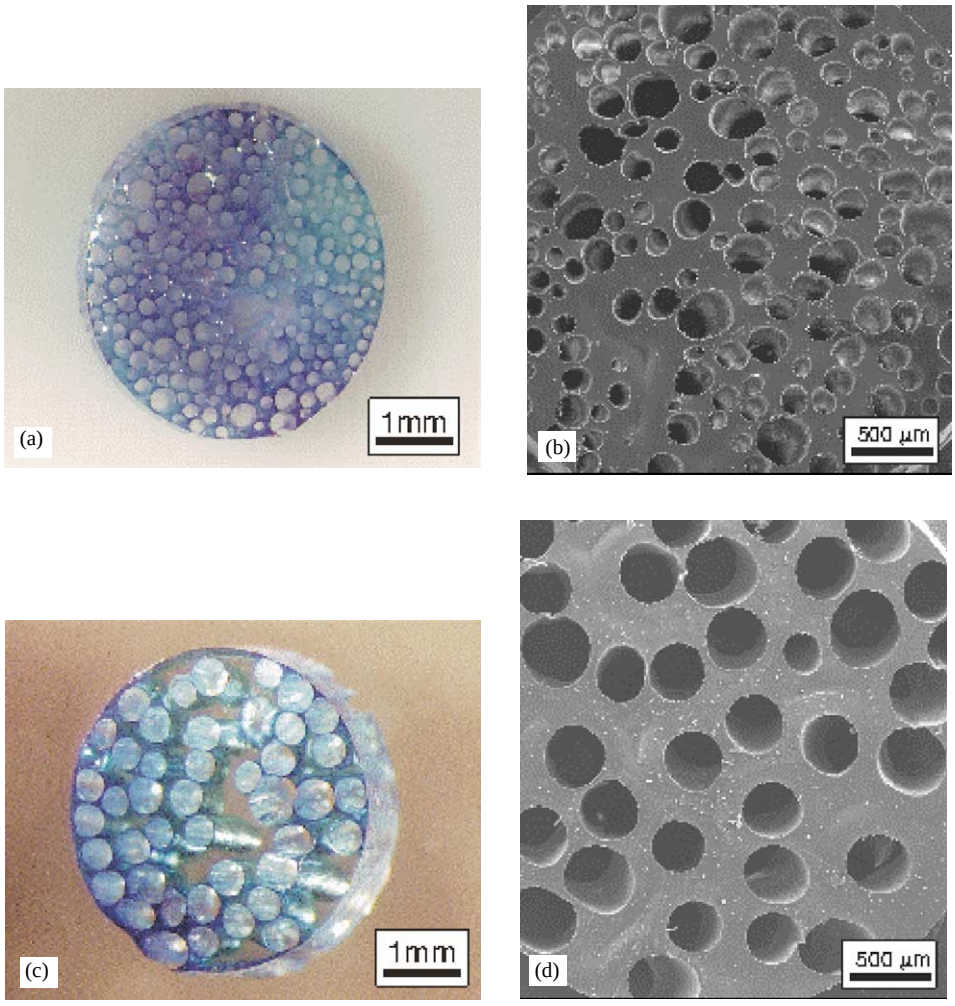

Fig. 1. Representative (a) optical (8 ×) and (b) electron micrographs of small channel scaffolds and (c) optical (8 ×) and (d) electron micrographs of large channel scaffolds.

beneficial to have many channels of different dimensions, thereby increasing the surface area available for regeneration, while at the same time minimizing the amount of polymer used and maximizing the space available to regenerating axons. While we have not yet investigated the optimal channel diameter, we [36] and others have observed neurite guidance on fibers with diameters of ~150 μm and less [33].

3.2. Channel diameter

In both the small and large channel scaffolds, a distribution in the diameter of the individual channels was observed due to variations in the diameters of the extruded PCL fibers. During the extrusion process, diameter fluctuations occurred as the fibers produced were extremely fine and the liquefied PCL was occasionally prone to breaking or stretching. A more controlled extrusion system would reduce the PCL fiber diameter variations, thereby narrowing the channel diameter distribution in the resultant scaffolds. The diameter of the small channels ranged from 50 to 300 μm, as shown in Fig. 2, with ~75% of the channels in the 100–200 μm diameter range. The large channel scaffolds were investigated to demonstrate the flexibility of the fiber dissolution system to produce oriented scaffolds with varying dimensions. In the large channel samples, the channel diameters ranged from 250 to 450 μm, as shown in Fig. 2, with ~77% of the channels in the 300–400 μm diameter range. Based on size alone, cellular invasion in both small and large diameter channels should be facile.

Based on average fiber counts and diameters, we estimated the increase of available surface area of a scaffold-filled vs. an empty hollow fiber membrane of similar dimensions. The small channel scaffolds, with an average channel diameter of approximately 152 μm and an average of 142 channels, augmented the surface area by an estimated 540% whereas the large channel scaffolds, with an average diameter of approximately 332 μm and an average of 32 channels, resulted in an estimated area increase of 310%. By mixing fiber sizes, a

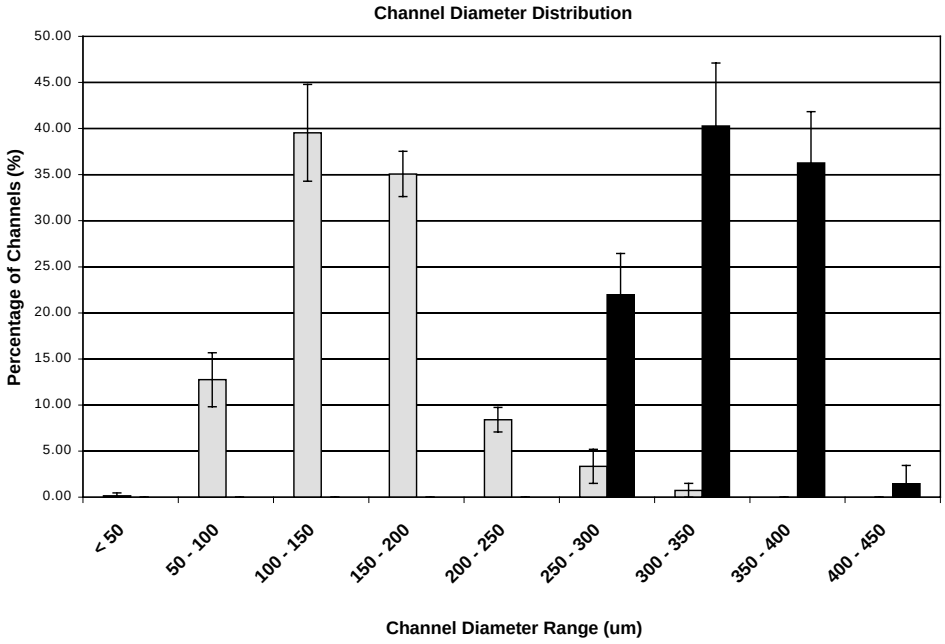

Fig. 2. Graph of the distribution of channel diameters for the (□) small channel scaffolds and (■) large channel scaffolds, expressed as a percentage of the total number of channels present. Approximately 130 channels were measured per small channel sample and approximately 30 channels were measured per large channel sample ($n = 6$; mean ± standard deviations are plotted).

higher density of channels and thus a greater increase in available surface area should be possible. Augmenting the surface area could significantly improve regeneration by promoting cell attachment and directional growth.

3.3. Scaffold porosity

Scaffold porosity was calculated, according to Eq. (1), by comparing the ratio of the area of the entire scaffold to that of the gel phase. In the small channel samples, the porosity was calculated to be $35 \pm 1\%$, while that of the large channel samples was $40 \pm 1\%$. Hence, although there were substantially fewer channels in the large samples, the increase in channel size resulted in the creation of a more porous scaffold due to a reduction in the amount of gel between the channels. The porosity calculation was also utilized to assess channel continuity and scaffold uniformity within individual samples. We calculated porosity at 3 different points along the length of each sample and found that it varied within 1% for the small channel scaffolds and 3% for the large channel scaffolds, thereby confirming that the channels were continuous and the structures were homogeneous.

3.4. Equilibrium water content

The EWC was calculated according to Eq. (2) and was $55.0 \pm 1.2\%$ for the small channel scaffolds and $56.2 \pm 2.9\%$ for the large channel scaffolds. These values are substantially higher than the $39.6 \pm 0.3\%$ EWC measured for transparent, non-perforated pHEMA gels of the same formulation. The elevation in EWC is likely due to the presence of water inside the scaffold channels, which could not be easily removed prior to weighing the wet mass.

3.5. Compressive modulus

The compressive modulus was 191 ± 7 kPa for the small channel scaffolds and 182 ± 4 kPa for the large channel scaffolds. Additionally, the modulus of the gel phase portion of each type of scaffold was calculated and compared to the expected value of approximately 290 kPa for transparent pHEMA gels [35]. By considering only the gel phase in our calculation of area, the gel phase moduli were determined to be 291 ± 11 and 301 ± 6 kPa for the small and large channel scaffolds, respectively, thereby confirming the accuracy of our experimental methods and the data reported.

The scaffold structures were strong, yet compliant and flexible, and had moduli comparable to that of the spinal cord, which is between 240 and 260 kPa for the feline model [37,38]. Matching the mechanical properties of the device to the site of implantation is important for success in in vivo applications. As with many tissue-engineered constructs, the scaffold must be strong enough to resist structural collapse upon implantation, but must not be so rigid as to damage the surrounding tissues, which may lead to inflammation and subsequent device failure [26,39].

4. Conclusions

Oriented pHEMA scaffolds were successfully fabricated using a fiber templating technique involving the solubilization of embedded PCL fibers dispersed in pHEMA gels. The process was safe, effective and reproducible, resulting in the production of scaffolds with highly controlled dimensions. Each scaffold had longitudinally oriented, fiber free channels that were continuous along the entire length of the structure. The size and arrangement of the PCL fibers in the transparent pHEMA controlled the diameter and patterning of the resultant channels. The channels may act as a bridge, providing support and contact guidance for extending axons and invading cells. These scaffolds may be useful for guided regeneration and we are investigating them for inclusion in a multi-component tissue engineered device to promote regeneration after transection injury in either the peripheral nerve or spinal cord.

Acknowledgements

We thank Ying Fang Chen for technical assistance. We gratefully acknowledge support from the Natural Sciences and Engineering Research Council of Canada.

References

[1] Battison B, Tos P, Cushway TR, Geuna S. Nerve repair by means of vein filled with muscle grafts I. Clinical results. Microsurgery 2000;20:32–6.
[2] Fry EJ. Central nervous system regeneration: mission impossible. Clin Exp Pharmacol Physiol 2001;28:253–8.
[3] Schwab ME. Regenerative nerve fiber growth in the adult central nervous system. News Physiol Sci 1998;13:294–8.
[4] Evans GRD. Peripheral nerve injury: a review and approach to tissue engineered constructs. Anat Rec 2002;263:396–404.
[5] Mackinnon SE, Dellon AL. Clinical nerve reconstruction with a bioabsorbable polyglycolic acid tube. Plastic Reconstructive Surg 1990;85:419–24.
[6] Meek MF, Den Dunnen WFA, Schakenraad JM, Robinson PH. Long-term evaluation of functional nerve recovery after reconstruction with a thin-walled biodegradable poly (DL-lactide-epsilon-caprolactone) nerve guide, using walking track analysis and electrostimulation tests. Microsurgery 1999;19:247–53.
[7] Li ST, Archibald SJ, Krarup C, Madison R. Peripheral nerve repair with collagen conduits. Clin Mater 1992;9:195–200.
[8] Dalton PD, Shoichet MS. Creating porous tubes by centrifugal forces for soft tissue applications. Biomaterials 2001;22:2661–9.
[9] Dalton PD, Flynn L, Shoichet MS. Manufacture of poly(2-hydroxyethyl methacrylate-co-methyl methacrylate) hydrogel tubes for use as nerve guidance channels. Biomaterials 2002;23:3843–51.
[10] Tsai EC, Dalton PD, Shoichet MS, Tator CH. Synthetic hydrogel guidance channels facilitate regeneration of adult rat brainstem motor axons after complete spinal cord transection. J Neurotrauma, submitted for publication.
[11] Midha R, Munroe CA, Dalton PD, Tator CH, Shoichet MS. Peripheral nerve regeneration through synthetic hydrogel nerve is enhanced by growth factors. Exp Neuroltube, accepted for publication.
[12] Dalton PD, Tsai E, Van Bendegem RL, Tator CH, Shoichet MS. Hydrogel nerve guides promote regeneration in the central nervous system. Tampa Bay, FL: Society for Biomaterials; 2002.
[13] Saneinejad S, Shoichet MS. Patterning poly(chlorotrifluoroethylene) to direct neuronal cell adhesion and process outgrowth. J Biomed Mater Res 2000;50:465–74.
[14] Cao X, Shoichet M. Defining the concentration gradient of nerve growth factor for guided neurite outgrowth. Neuroscience 2001;103:831–40.
[15] Kapur TA, Shoichet MS. Chemically bound growth factors for nerve tissue engineering. J Biomater Sci: Polym Ed, in press.
[16] Letourneau P. Axonal growth and guidance. Trends Neurosci 1983;6:451–5.
[17] Dubey N, Letourneau PC, Tranquillo RT. Guided neurite elongation and Schwann cell invasion into magnetically aligned collagen in simulated peripheral nerve regeneration. Exp Neurol 1999;158:338–50.
[18] Ceballos D, Navarro X, Dubey N, Wendelshafer-Crabb G, Kennedy WR, Tranquillo RT. Magnetically aligned collagen gel filling a collagen nerve guide improves peripheral nerve regeneration. Exp Neurol 1999;158:290–300.
[19] Yoshii S, Oka M. Collagen filaments as a scaffold for nerve regeneration. J Biomed Mater Res 2001;56:400–5.
[20] Chauhan NB, Figlewicz HM, Khan T. Carbon filaments direct the growth of postlesional plastic axons after spinal cord injury. Int J Dev Neurosci 1999;3:255–64.
[21] Rangappa N, Romero A, Nelson KD, Eberhart RC, Smith GM. Laminin-coated poly(L-lactide) filaments induce robust neurite growth while providing directional orientation. J Biomed Mater Res 2000;51:625–34.
[22] Terada N, Bjursten LM, Papaloizos M, Lundborg G. Resorbable filament structures as a scaffold for matrix formation and axonal growth in bioartificial nerve grafts: long term observations. Restorative Neurol Neurosci 1997;11:65–9.
[23] Hadlock T, Elisseeff J, Langer R, Vacanti J, Cheney M. A tissue-engineering conduit for peripheral nerve repair. Arch Otolaryngol Head Neck Surg 1998;124:1081–6.
[24] Ma PX, Zhang R. Microtubular architecture of biodegradable polymer scaffolds. J Biomed Mater Res 2001;56:469–77.
[25] Hoffman AS. Hydrogels for biomedical applications. Adv Drug Del Rev 2002;43:3–12.
[26] Peppas NA, Huang Y, Torres-Lugo M, Ward JH, Zhang J. Physiochemical foundations and structural design of hydrogels in medicine and biology. Annu Rev Biomed Eng 2000;2:9–29.
[27] Park H, Park K. Hydrogels in bioapplications. ACS Symp Ser 1996;627:2–10.
[28] Chirila TV, Chen YC, Griffin BJ, Constable IJ. Hydrophilic sponges based on 2-hydroxyethyl methacrylate. 1. Effect of monomer mixture on the pore size. Polym Int 1993;32:221–32.
[29] Nicolson PC, Vogt J. Soft contact lenses polymers: an evolution. Biomaterials 2001;22:3273–83.
[30] Chirila TV, Higgins B, Dalton PD. The effect of synthesis conditions on the properties of poly(2-hydroxyethyl methacrylate) sponges. Cell Polym 1998;17:141–62.
[31] Hicks CR, Crawford G, Chirila TV, Wiffen S, Vijayasekeran S, Lou X, Fitton J, Maley M, Clayton A, Dalton P, Platten S, Ziegelaar B, Hong Y, Russo A, Constable I. Development and

clinical assessment of an artificial cornea. Prog Retinal Eye Res 2000;19:149–70.

[32] Hicks CR, Clayton AB, Vijayasekeran S, Crawford GJ, Chirila TV, Constable IJ. Development of a poly(2-hydroxyethyl methacrylate) orbital implant allowing direct muscle attachment and tissue ingrowth. Ophthal Plastic Reconstructive Surg 1999;15:326–32.

[33] Smeal RM, Rabbitt RD, Tresco PA. Substrate curvature restricts the directional outgrowth of dorsal root ganglion cells: implantations for development. 30th Annual Meeting Transactions, Society for Neuroscience, 2000.

[34] Kapur TA, Shoichet MS. Immobilized concentration gradients of nerve growth factor guide neurite outgrowth. J Biomed Mater Res, accepted for publication.

[35] Johnson B, Niedermaier DJ, Crone WC, Moorthy J, Beebe DJ. Mechanical properties of a pH sensitive hydrogel. 2002 SEM Annual Conference Proceedings, Milwaukee, WI.

[36] Shoichet MS, Shaw D. Peptide-modified ePTFE fibers guide axonal elongation. J Craniofacial Surg, in press.

[37] Chang GL, Hung TK, Feng WW. An in vivo measurement and analysis of viscoelastic properties of the spinal cord of cats. J Biomech Eng 1988;110:115–22.

[38] Hung TK, Chang GL, Lin HS, Walter FR, Bunegin L. Stress–strain relationship of the spinal cord of anesthetized cats. J Biomech 1980;14:269–76.

[39] Greenwald SE, Berry CL. Improving vascular grafts: the importance of mechanical and haemodynamic properties. J Pathol 2000;190:292–9.